INTERNATIONAL JOURNAL OF
NUMERICAL ANALYSIS AND MODELING, *SERIES B*
Volume 3, Number 2, Pages 192–206

AN ENHANCED MATHEMATICAL MODEL FOR PHASE CHANGE PROBLEMS WITH NATURAL CONVECTION

YOUSSEF BELHAMADIA, ABDOULAYE S. KANE, AND ANDRÉ FORTIN

Abstract. The enthalpy-porosity technique is commonly used for modeling phase change problems with natural convection. In most applications however, this technique is restricted to equal thermophysical properties of solid and liquid phases. In this paper, an enhanced formulation based on the enthalpy-porosity method is proposed where the different thermophysical properties between the two phases can be easily taken into account. Accurate temporal and spatial discretizations are also presented for solving the proposed formulation. Numerical simulations on pure gallium melting and a comparison between experimental and numerical results for water solidification are presented to illustrate the performance of the proposed model and numerical methodology.

Key words. Phase change problems with natural convection, mixed finite element formulation, interface liquid-solid, gallium melting, and water solidification

1. Introduction

Phase change problems with natural convection play a significant role in several industrial applications. The main challenge of such problems is the presence of a moving liquid-solid interface involving a strong coupling of mass and heat transfer. The mathematical models for solving phase change with convection can be roughly divided into two categories. The first one is based on a multi-domain approach where the momentum and energy equations are solved in each phase domain separately (see Florez et al. [10], Gupta [14], Viswanath and Jaluria [23], and the references therein). This approach thus requires a continuous update of the two domains due to the time dependent interface position. The second category is based on a single-domain approach where a system of momentum and energy equations is solved in the entire physical domain (see Rady and Mohanty [19], Samarskii et al. [20], Voller and Prakash [25], and the references therein). The main advantage of this approach is that the interface is not explicitly computed and the energy balance condition is automatically satisfied at the interface.

The enthalpy-porosity model is widely used as a single domain approach (see Brent et al. [5] and Voller et al. [24]). This model includes latent heat effects as a source term and includes a technique to ensure that the velocity field vanishes in the solid region. This model is however mostly used when the thermophysical properties of solid and liquid are equal (see Hannoun et al. [16, 15] and Evans et al. [9], Evans and Knoll [8]). In the more general case, the enthalpy-porosity model can be reformulated into a vorticity-velocity model. This formulation is based on averaging the physical variables velocity, density, and thermal conductivity, by using liquid-solid mass and volume fraction. The reader is referred to Kowalewski and Rebow [18], and Giangi et al. [12, 13] for a more detailed description.

Phase change problems including natural convection are challenging from a numerical point of view. Small time steps and very fine meshes as well as accurate space and time discretizations are required if one wants to capture the complex

Received by the editors February 7, 2012 and, in revised form May 20, 2012.
2000 *Mathematics Subject Classification.* 80A20, 80A22, 80M10, 65M60, 76D05.

physics of the problem and especially to accurately compute the liquid-solid interface where phase change occurs. Indeed, the use of second order accurate spatial discretizations on tin and gallium melting problems have been investigated in Hannoun et al. [16] and it is concluded that second order accuracy as well as fine meshes are required to obtain the proper number and location of roll cells. The mesh dependence of the flow structure of pure gallium melting was put in evidence in Stella and Giangi [21]. However, only first order fully implicit time discretizations have been tested in these previous works. To our knowledge, the issue of time discretization accuracy for phase change convection simulations has been addressed only in Evans and Knoll [8] where temporal accuracy analysis using a Jacobian-free Newton-Krylov (JFNK) solution method with a pressure-correction smoother (SIMPLE) algorithm is performed for the non-dimensional solidification test case and pure gallium melting problems.

Phase change problems have enormous importance in many engineering and industrial processes. Freezing of water is an example that has recently received a lot of experimental and numerical attention. In Kowalewski and Rebow [17, 18], an experimental benchmark was set up to study the transient natural convection during freezing of water in a cube-shaped cavity. The experimental data was compared to numerical results performed with a finite difference method and using the multi-domain approach where the governing equations are solved separately for the fluid and solid domain. Important discrepancies were observed in the interface position and flow patterns. In Giangi et al. [12, 13] numerical and experimental results were also presented based on a similar freezing of water problem. This time, the numerical results were obtained using a finite volume method and a vorticity-velocity model. Discrepancies between numerical and experimental results were again reported despite the fact that the mesh dependance and the effects of thermal boundary conditions were closely analyzed. Similar discrepancies for water solidification has been also reported in Banaszek et al. [1]. A semi-implicit finite element method was adopted for the two-dimensional simulation and the mathematical model was based on the general enthalpy formula as presented in Swaminathan and Voller [22].

In a previous work of the authors, a finite element formulation has been introduced for phase change problems without convection. This formulation considers both equal and different liquid-solid physical properties and has been validated on various two and three dimensional problems (see Belhamadia et al. [2, 3], Fortin and Belhamadia [11]). The main goal of this work is first to present a more general form of this formulation in order to include the presence of natural convection. The proposed formulation is based on an enthalpy-porosity model and allows us to consider the case where liquid and solid physical properties differs. A fully implicit finite element mixed formulation for both the momentum and energy equations is also proposed. The discretization is second order accurate in both space and time. The advantage and performance of the overall technique are analyzed on two classical benchmark problems: pure gallium melting where our numerical solutions are compared with the existing literature results and water solidification where a comparison between experimental and numerical results is performed showing that the above mentioned discrepancies are clearly reduced when using the proposed method.

The organization of this paper is as follows. In Section II, the enthalpy-porosity model is briefly recalled and the proposed model is introduced. Section III is devoted to the numerical method and finite element discretization. Finally, section IV presents numerical results showing the performance of the proposed method.

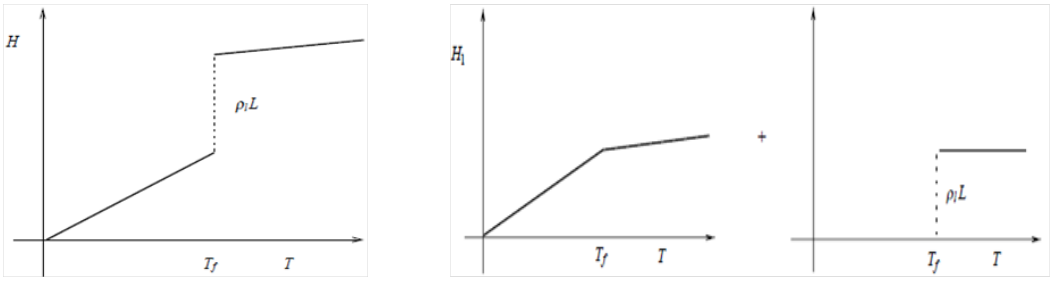

a) Enthalpy-Temperature relation b) Relation $H = H_1 + \rho_l L\phi$

FIGURE 1. Enthalpy and Temperature

2. Mathematical Model

Under the assumption that the fluid is Newtonian and incompressible, the enthalpy-porosity governing equation (see [5] and [24]) can be written as:
Conservation of momentum

$$\rho_l \frac{\partial \boldsymbol{u}}{\partial t} + \rho_l \boldsymbol{u} \cdot \nabla \boldsymbol{u} = \nabla \cdot (2\mu \dot{\boldsymbol{\gamma}}(\boldsymbol{u})) - \nabla p + A\boldsymbol{u} + S(H)$$

Conservation of mass

$$\nabla \cdot \boldsymbol{u} = 0$$

Conservation of energy

$$\frac{\partial H}{\partial t} + \boldsymbol{u} \cdot \nabla H - \nabla \cdot (\boldsymbol{K} \nabla T) = 0$$

where $\boldsymbol{u}$ is the velocity, $\dot{\boldsymbol{\gamma}}(\boldsymbol{u}) = \dfrac{(\nabla \boldsymbol{u} + \nabla \boldsymbol{u}^T)}{2}$ is the symmetric part of the velocity gradient tensor, p is the pressure, H is the enthalpy, T is the temperature, μ is the viscosity, ρ_l is the liquid density, and $\boldsymbol{K}$ is the conductivity tensor. A is defined so that the momentum equations are forced to mimic the Carman-Kozeny equations,

$$A = -C \frac{(1-\varepsilon)^2}{\varepsilon^3 + b} \tag{1}$$

where C is a constant accounting for the mushy-region morphology, ε is the porosity between 0 and 1 and $b = 10^{-6}$ is a constant introduced to avoid division by zero. As can be seen from (1), A vanishes in the fluid and has no influence therein. In totally solid region however, A takes a large value and forces the velocity field to vanish.

Assuming the Boussinesq approximation, the gravity source term can be written as

$$S(H) = \frac{\beta(H - H_{\text{ref}})}{c_l} \boldsymbol{g}$$

where c_l is the liquid specific heat, $\boldsymbol{g}$ the acceleration vector due to gravity and H_{ref} is a reference value for the enthalpy.

We now consider the general case where the thermophysical properties of solid and liquid may be different. The formulation is derived from enthalpy-porosity model by considering the following general formula of the enthalpy (see Figure 1a)):

$$H = \begin{cases} H_s = \rho_s c_s T & \text{if} \quad T < T_f, \\ H_l = \rho_l L + \rho_s c_s T_f + \rho_l c_l (T - T_f) & \text{if} \quad T > T_f. \end{cases}$$

where L is the latent heat of fusion. As in [2, 3], a phase change variable ϕ is introduced as:

$$\phi = \begin{cases} 0 & \text{in } \Omega_s, \\ 1 & \text{in } \Omega_l. \end{cases} \tag{2}$$

As can be seen in Figure 1b), the enthalpy can be decomposed as:

$$H = H_1 + \rho_l L \phi,$$

where H_1 is now a continuous function:

$$H_1 = \begin{cases} \rho_s c_s T & \text{in } \Omega_s, \\ \rho_s c_s T_f + \rho_l c_l (T - T_f) & \text{in } \Omega_l, \end{cases}$$

so that

$$\frac{\partial H_1}{\partial t} = \begin{cases} \rho_s c_s \frac{\partial T}{\partial t} & \text{in } \Omega_s, \\ \rho_l c_l \frac{\partial T}{\partial t} & \text{in } \Omega_l. \end{cases} \text{ and } \frac{\partial H_1}{\partial \mathbf{x}} = \begin{cases} \rho_s c_s \frac{\partial T}{\partial \mathbf{x}} & \text{in } \Omega_s, \\ \rho_l c_l \frac{\partial T}{\partial \mathbf{x}} & \text{in } \Omega_l. \end{cases}$$

Now the energy equation

$$\frac{\partial H}{\partial t} + \boldsymbol{u} \cdot \nabla H - \nabla \cdot (\boldsymbol{K} \nabla T) = 0,$$

becomes

$$\alpha(\phi) \frac{\partial T}{\partial t} + \alpha(\phi) (\boldsymbol{u} \cdot \nabla T) + \rho_l L \frac{\partial \phi}{\partial t} + \rho_l L (\boldsymbol{u} \cdot \nabla \phi) - \nabla \cdot (\boldsymbol{K}(\phi) \nabla T) = 0, \tag{3}$$

or more compactly

$$\alpha(\phi) \frac{DT}{Dt} + \rho_l L \frac{D\phi}{Dt} - \nabla \cdot (\boldsymbol{K}(\phi) \nabla T) = 0,$$

where $\frac{D}{Dt}$ is the total derivative and:

$$\begin{cases} \alpha(\phi) &= \rho_s c_s + \phi (\rho_l c_l - \rho_s c_s), \\ \boldsymbol{K}(\phi) &= \boldsymbol{K}_s + \phi (\boldsymbol{K}_l - \boldsymbol{K}_s), \\ f(\phi) &= f_s + \phi (f_l - f_s). \end{cases}$$

and the function ϕ satisfies a simple algebraic equation of the form:

$$\phi = F(T) = \begin{cases} 0 & \text{if } T < T_f, \\ 1 & \text{if } T > T_f, \end{cases}$$

Thus A and S can written as

$$A(\phi) = -C \frac{(1-\phi)^2}{\phi^3 + b} \text{ and } S(T) = \rho_l \beta (T - T_{\text{ref}}) \boldsymbol{g}$$

where T_{ref} is a reference temperature that will be set in the numerical simulation section. As mentioned in [5], in the case of isothermal phase change, the term $\rho_l L (\boldsymbol{V} \cdot \nabla \phi)$ vanishes. Moreover, in applications, phase change is not always instantaneous and may occur in a small temperature range $[T_f - \epsilon, T_f + \epsilon]$. The relation for $F(T)$ can thus be replaced by a regularized one ($F_\epsilon(T)$) and it can be done in a number of more or less efficient ways. The idea is to connect the constant value 0 (for $T < T_f - \epsilon$) and the constant value 1 (for $T > T_f + \epsilon$) by a cubic Hermite polynomial and therefore the resulting curve is differentiable as long as

$\epsilon \neq 0$. The functions α, $\boldsymbol{K}$, and f are then automatically regularized in a similar way since they depend on ϕ.

The proposed equations for phase change with natural convection can now be written as:

$$
\left\{
\begin{array}{l}
\rho_l \dfrac{\partial \boldsymbol{u}}{\partial t} + \rho_l \boldsymbol{u} \cdot \nabla \boldsymbol{u} = \nabla \cdot (2\mu \dot{\boldsymbol{\gamma}}(\boldsymbol{u})) - \nabla p + A(\phi)\boldsymbol{u} + S(T) \\
\nabla \cdot \boldsymbol{u} = 0 \\
\alpha(\phi) \dfrac{DT}{Dt} + \rho L \dfrac{D\phi}{Dt} - \nabla \cdot (\boldsymbol{K}(\phi) \nabla T) = 0, \\
\phi = F_\epsilon(T).
\end{array}
\right. \tag{4}
$$

3. Finite element discretization

A mixed (velocity-pressure) formulation for Navier-Stokes equations is used. The finite element discretization is based on quadratic polynomials (written using a hierarchical basis) for the velocity and linear (continuous) polynomials for the pressure. This discretization is second order accurate in space ($O(h^2)$) as shown in Brezzi and Fortin [6]. To simplify the presentation of the variational formulation, homogeneous boundary conditions are imposed for all the variables but the general case follows the same lines. Using the test functions $(\boldsymbol{v_u}, v_p)$, we have:

$$
\left\{
\begin{array}{l}
\displaystyle\int_\Omega \left(\rho_l \frac{\partial \boldsymbol{u}}{\partial t} \cdot \boldsymbol{v_u} + \rho_l \left(\boldsymbol{u} \cdot \nabla \boldsymbol{u} \right) \cdot \boldsymbol{v_u} \right) d\Omega \\
\displaystyle + \int_\Omega \left(2\mu \dot{\boldsymbol{\gamma}}(\boldsymbol{u}) : \dot{\boldsymbol{\gamma}}(\boldsymbol{v_u}) - p \nabla \cdot \boldsymbol{v_u} - A(\phi)\boldsymbol{u} \cdot \boldsymbol{v_u} \right) d\Omega = \int_\Omega S(T) \cdot \boldsymbol{v_u} d\Omega, \\
\displaystyle\int_\Omega v_p \nabla \cdot \boldsymbol{u} d\Omega = 0.
\end{array}
\right.
$$

A mixed formulation is also employed for the energy equation. The formulation was successfully employed for phase change problem without convection (see Belhamadia et al. [2, 3]). The finite element discretization is based on quadratic polynomials for both the temperature T and phase change variable ϕ and is therefore also second order accurate in space ($O(h^2)$). The corresponding variational formulation is obtained by multiplying the energy equations by the test functions (v_T, v_ϕ) and can be written as:

$$
\left\{
\begin{array}{l}
\displaystyle\int_\Omega \left(\alpha(\phi) \frac{\partial T}{\partial t} v_T + \alpha(\phi) \left(\boldsymbol{u} \cdot \nabla T \right) v_T \right) d\Omega + \int_\Omega \left(\rho_l L \frac{\partial \phi}{\partial t} v_T + \rho_l L \left(\boldsymbol{u} \cdot \nabla \phi \right) v_T \right) d\Omega \\
\qquad\qquad \displaystyle + \int_\Omega \left((\boldsymbol{K}(\phi) \boldsymbol{\nabla} T) \cdot \boldsymbol{\nabla} v_T \right) d\Omega = 0, \\
\displaystyle\int_\Omega (\phi - F_\epsilon(T)) v_\phi \, d\Omega = 0.
\end{array}
\right.
$$

In all our numerical simulations, a fully implicit backward second order scheme (also known as Gear or BDF2 in the literature) is employed for time discretization. For instance, given approximate solutions $\boldsymbol{u}^{n-1}$, $\boldsymbol{u}^n$ and $\boldsymbol{u}^{n+1}$ at times t^{n-1}, t^n and t^{n+1}, respectively, the time derivative at time t^{n+1} is approximated by:

$$
\frac{\partial \boldsymbol{u}}{\partial t}(t^{(n+1)}) \simeq \frac{3\boldsymbol{u}^{(n+1)} - 4\boldsymbol{u}^{(n)} + \boldsymbol{u}^{(n-1)}}{2\Delta t}.
$$

Therefore the overall algorithm for solving the proposed model is the following:

(1) Starting from a solution $(T^{(n)}, \phi^{(n)})$, the approximations $(u^{(n+1)}, p^{(n+1)})$ are obtained based on the following system

$$\begin{cases} \displaystyle\int_\Omega \left(\rho_l \frac{3\boldsymbol{u}^{(n+1)} - 4\boldsymbol{u}^{(n)} + \boldsymbol{u}^{(n-1)}}{2\Delta t} \cdot \boldsymbol{v_u}\right) d\Omega \\ \displaystyle + \int_\Omega \left(\rho_l \left(\boldsymbol{U} \cdot \nabla \boldsymbol{u}^{(n+1)}\right) \cdot \boldsymbol{v_u} + 2\mu \dot{\boldsymbol{\gamma}}(\boldsymbol{u})^{(n+1)} : \dot{\boldsymbol{\gamma}}(\boldsymbol{v_u})\right) d\Omega \\ \displaystyle + \int_\Omega \left(-p^{(n+1)} \nabla \cdot \boldsymbol{v_u} - A(\phi^{(n)}) \boldsymbol{u}^{(n+1)} \cdot \boldsymbol{v_u}\right) d\Omega = \int_\Omega S(T^{(n)}) \cdot \boldsymbol{v_u} d\Omega, \\ \displaystyle \int_\Omega v_p \nabla \cdot \boldsymbol{u}^{(n+1)} d\Omega = 0, \end{cases}$$

(2) Starting from the solutions $(u^{(n+1)}, p^{(n+1)})$, the approximations $(T^{(n+1)}, \phi^{(n+1)})$ are obtained based on the following system

$$\begin{cases} \displaystyle\int_\Omega \left(\alpha(\phi^{(n+1)}) \frac{3T^{(n+1)} - 4T^{(n)} + T^{(n-1)}}{2\Delta t} v_T\right) d\Omega \\ \displaystyle + \int_\Omega \left(\alpha(\phi^{(n+1)}) \left(\boldsymbol{u}^{(n+1)} \cdot \nabla T^{(n+1)}\right) v_T\right) d\Omega \\ \displaystyle + \int_\Omega \left(\rho_l L \frac{3\phi^{(n+1)} - 4\phi^{(n)} + \phi^{(n-1)}}{2\Delta t} v_T\right) d\Omega + \int_\Omega \left(\rho_l L \left(\boldsymbol{u}^{(n+1)} \cdot \nabla \phi^{(n+1)}\right) v_T\right) d\Omega \\ \displaystyle + \int_\Omega \left((\boldsymbol{K}(\phi^{(n+1)}) \boldsymbol{\nabla} T^{(n+1)}) \cdot \boldsymbol{\nabla} v_T\right) d\Omega = 0, \\ \displaystyle \int_\Omega (\phi^{(n+1)} - F_\epsilon(T^{(n+1)})) v_\phi \, d\Omega = 0. \end{cases}$$

(3) Return to step (1).

Where $\boldsymbol{U}$ in step (1) can be $\boldsymbol{u}^{(n+1)}$ and therefore Newton's method must be used to linearize the system. A better and less expensive method consists in extrapolating U from previous time steps. The simplest possibility is to set $U = \boldsymbol{u}^{(n)}$ in a Picard iterative scheme. An even more efficient method is the Richardson extrapolation where $U = 2\boldsymbol{u}^{(n)} - \boldsymbol{u}^{(n-1)}$. In addition, as the extrapolation $2T^{(n)} - T^{(n-1)}$ is a second order approximation of $T^{(n+1)}$, it would probably be a better choice to replace the term $S(T^n)$ by $S(2T^{(n)} - T^{(n-1)})$. The same conclusion is true for $A(\phi^{(n)})$ but this was not done in the present work. In step (2), the non linear system is solved at each time step with Newton's method. In all cases, an efficient preconditioned iterative solver developed in El Maliki and Guénette [7] is employed for the quadratic discretization arising from the linearized incompressible Navier-Stokes equations.

Note that the momentum system in step (1) can be solved without including the term $A(\phi^{(n)})\mathrm{u}^{(n+1)}$ in the variational formulation. This can be done by imposing a null Dirichlet boundary condition in the fluid region identified by the condition $\phi^{(n)} \geq 0.99$. Our numerical results show that this is equivalent to using the term $A(\phi) = -C\dfrac{(1-\phi)^2}{\phi^3 + b}$ with a large value of C.

4. Numerical Results

To assess the reliability and accuracy of the proposed formulation and discretizations, two benchmark problems will be employed. The first one considers pure gallium melting and the second considers water solidification.

4.1. Melting of pure Gallium. Although the physical proprieties of gallium are equal in both liquid and solid phases, the problem of gallium melting in a rectangular cavity heated from one side is our first test since it is extensively used in the literature for the assessment of phase-change numerical methods. The problem consists of a two-dimensional cavity $[0, 3.175] \times [0, 6.35]$cm. The left side temperature is maintained fixed at $T_h = 311K$ and the right side temperature is $T_c = 301.3K$, while homogeneous Neumann conditions are imposed on all the other sides. All the other physical proprieties are provided in Evans and Knoll [8] and Hannoun et al. [16] and are the following:

μ	$1.81 \times 10^{-3}(\mathrm{Ns}/(\mathrm{m}^2))$,
g	$10(\mathrm{m}/\mathrm{s}^2)$,
β	$1.2 \times 10^{-4}, (\mathrm{K}^{-1})$
$\rho_l = \rho_s$	$6093.0\left(\mathrm{kg}/\mathrm{m}^3\right)$,
$c_l = c_s$	$381.5\,(\mathrm{J}/\mathrm{kg\,K})$,
$\boldsymbol{K}_l = \boldsymbol{K}_s$	$32.0\boldsymbol{I}\,(\mathrm{W}/\mathrm{m\,K})$,
L	$80160.0\,(\mathrm{J}/\mathrm{kg})$,
T_f	302.78(K).
T_{ref}	301.3(K).
C	10^{15}

The corresponding dimensionless parameters are the Prandtl number $Pr = 0.0216$, the Rayleigh number $Ra = 7 \times 10^5$ and the Stefan number $Ste = 0.046$.

It is well known that phase change problems are very sensitive to time step and mesh sizes. A complete mesh sensitivity analysis for melting of pure Gallium has been performed in Stella and Giangi [21]. Similar results have been obtained in Hannoun et al. [16] where a central finite volume method with a fully implicit Euler method for time discretization were used. The numerical results were obtained with a uniform mesh of step size of $h = 0.01$cm and time steps varying from 0.1s to 0.01s (decreasing as melting proceeds).

In this paper, two uniform meshes of space step size $h = 0.03$cm, and $h = 0.015$cm are employed using a large fixed time step size of $\Delta t = 0.2$s. Figure 2 and 3 show the time evolution of the solid liquid interface as well as the streamlines using the two meshes. The results using $h = 0.015$cm are in excellent agreement with the results of [21] and [16] even though relatively large time step and space step size were used (see Figure 3). In this way, the enormous requirement in computational time can be reduced and this is made possible by time and space formulation employed in this paper.

The sensitivity to mesh size is clearly demonstrated in Figure 2 where numerical results with $h = 0.03$cm are presented. As can be seen, differences in cells number and form are observed from time $t = 36$s.

4.2. Water Solidification. Freezing of water is a very common phase change problem but it is still an interesting test case for the proposed formulation and finite element discretization since the physical parameters are different in each phase. A convective flow in a cubic box filled with pure distilled water is therefore considered. The inner dimension of the box is 38 mm. The right wall temperature is maintained

a) $t = 20$s b) $t = 32$s a) $t = 36$s b) $t = 42$s b) $t = 85$s

FIGURE 2. Simulation with $h = 0.03$cm

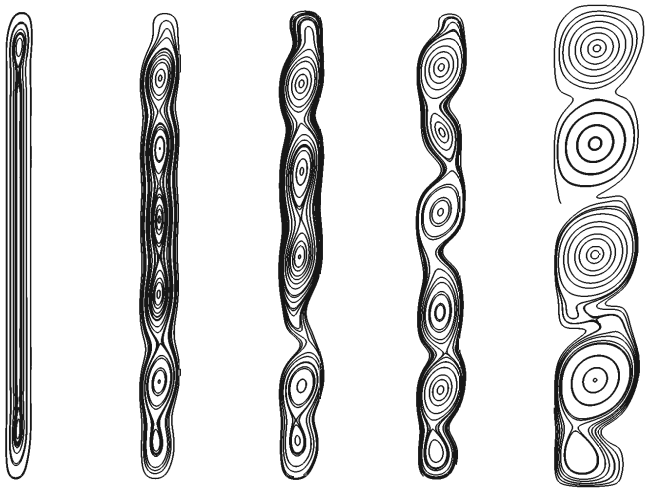

a) $t = 20$s b) $t = 32$s a) $t = 36$s b) $t = 42$s b) $t = 85$s

FIGURE 3. Simulation with $h = 0.015$cm

at $T_c = -10^{\circ}C$ and the opposite wall is held at a temperature $T_h = 10^{\circ}C$. The other four walls allow the entry of heat from the external fluid which surrounds the cavity and were made of 6mm thick Plexiglas. This problem has been widely investigated experimentally and numerically in the literature and the reader is refereed to Kowalewski and Rebow [18], and Giangi et al. [12, 13] and the references therein for more details.

A modified Boussinesq approximation is considered to include the non-linear variation of the water density and thus the gravity source term will have the form

$S(T) = -(\rho(T) - \rho_0)\mathbf{g}$, where the water density function $\rho(T)$ is given by

$$\begin{aligned}\rho(T) &= 999.840281167 + 0.0673268037314 \cdot T \\ &\quad -0.00894484552601 \cdot T^2 + 8.78462866500 \cdot 10^{-5} T^3 \\ &\quad +6.62139792627 \cdot 10^{-7} \cdot T^4\end{aligned}$$

with $\rho_0 = 999.84$. The remaining physical parameters are constant but different in each phase and are given in the following table:

μ	$1.79 \times 10^{(-6)}(\mathrm{Ns}/(\mathrm{m}^2))$,
ρ_s	$916.8\,(\mathrm{kg}/\mathrm{m}^3)$,
ρ_l	$999.84\,(\mathrm{kg}/\mathrm{m}^3)$,
c_s	$2116\,(\mathrm{J}/\mathrm{kg\,C})$,
c_l	$4202\,(\mathrm{J}/\mathrm{kg\,C})$,
$\boldsymbol{K}_s$	$2.26\boldsymbol{I}\,(\mathrm{W}/\mathrm{m\,C})$,
$\boldsymbol{K}_l$	$0.56\boldsymbol{I}\,(\mathrm{W}/\mathrm{m\,C})$,
L	$335000\,(\mathrm{J}/\mathrm{kg})$,
T_f	0(C).
T_0	0.5(C).
T_{ext}	25(C).

The corresponding non-dimensional numbers describing the investigated configuration are based on the fluid properties and their values are $Pr = 13.3$, $Ra = 1.503 \times 10^6$ and $Ste = 0.125$.

In the experimental results, ice front remains almost perpendicular to the bottom wall as presented in [18] (see figure 6a) on page 204). However, in all the numerical results presented in [17, 18, 12, 13], important discrepancies in the ice front form are observed and these differences are more pronounced when the freezing time exceeds 500s. In these contributions, two different types of boundary conditions were used. In the first approach, a homogeneous Neumann condition is imposed on non-isothermal walls while in the second approach, an additional energy equation for the 6mm Plexiglas side walls has been incorporated into the numerical model. Figure 4 illustrates these discrepancies at time $2500s$ where the numerical simulations has been obtained with the second boundary conditions approach using a second order finite difference approximation for spatial derivatives and forward Euler approximation in time. Discrepancies in the ice front form are also observed in [1] despite the fact that the mathematical model adopted was based on the general enthalpy formula that is similar to our approach. The performance of our method is however clearly presented in Belhamadia et al. [4] where a comparison with the numerical and experimental data from [1] has been employed.

Our simulations were performed with 30^3 mesh points and the interface position was determined by $T_f = 0$ (corresponding to $\phi = 0.5$). The liquid-solid interface and the velocity vectors at time $t = 2500s$ are presented in Figure 5. Only the first boundary condition approach (homogeneous Neumann) was employed. Figure 6 presents the interface positions at times, $t = 500$, $t = 1000s$, $t = 1500$, $t = 2000s$, and $t = 2500$ and as can be seen, the interface remains almost perpendicular to the bottom wall. A cross section of the interface position in the plane $z = 0.5$ at time 2500s is plotted in Figure 7 and compared with experimental data.

We believe that our simulations, as shown in Figure 7, can be even closer to the experimental data based on two main reasons. Firstly, it is not obvious how the experimental ice front is defined. Normally the solid-liquid interface is numerically

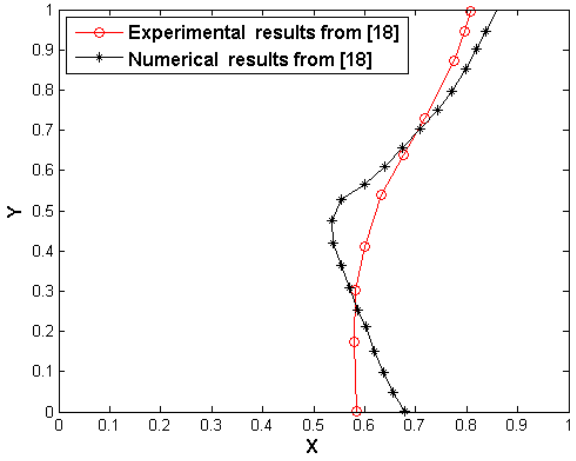

FIGURE 4. Comparison between numerical and experimental results from [18]

determined by the melting temperature $T_f = 0$ or $\phi = 0.5$. However, in all single-domain models, the momentum equations are solved only in the liquid region where ϕ is close to one and therefore the experimental ice front may not correspond to $\phi = 0.5$. The difference between the interface $\phi = 0.5$ and the ice front corresponding to $\phi = 0.8$ is illustrated in Figure 8 and compared to the experimental ice front from [18]. The differences are once again greatly reduced showing the necessity of a proper definition of the ice front.

Secondly, as presented in section 4.1, phase change problems are very sensitive to mesh size and this is particularly true for the interface position which may be strongly affected by mesh accuracy. Figure 9 shows two front positions, $\phi = 0.8$, obtained with two different meshes: the first with 20^3 mesh points or 48000 tetrahedral elements leading to 216024 dof for the momentum equations and 137842 dof for phase change equations and the second with 30^3 mesh points or 162000 tetrahedral elements leading to 710704 dof for the momentum equations and 453962 dof for phase change equations. The numerical solutions performed with the two meshes have been compared to the experimental front from [18]. The front position is clearly affected by the mesh resolution and therefore finer meshes or adapted meshes would probably be necessary.

The comparison between numerical and experimental for freezing of water presented in this work is very promising and it has the advantage to preserve the interface form showing the performance of the suggested methodology.

5. Conclusion

In this paper, an enhanced model for phase change problem with convection is presented. In this model, the different physical properties of the liquid and solid phases are easily introduced and implemented. Accurate temporal and spacial discretizations were introduced for solving the proposed formulation.

The overall technique has been first employed for pure gallium melting problem. The results obtained are in good agreement with existing literature numerical results even though a larger time and space step sizes were used. The proposed model

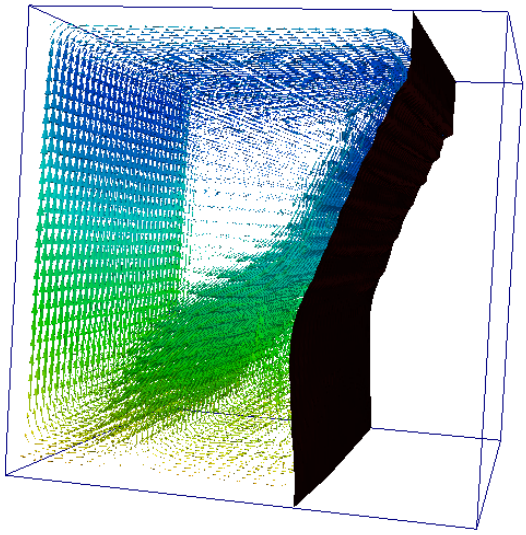

FIGURE 5. Liquid-solid interface and velocity vectors at time $t = 2500s$

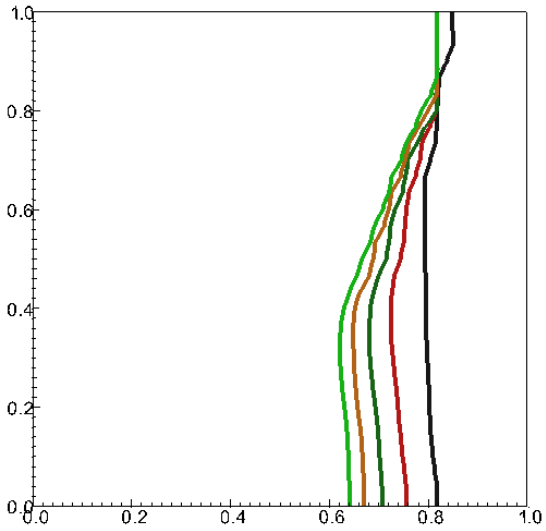

a) Interface evolution at different times:
$t = 500$, $t = 1000s$, $t = 1500$, $t = 2000$, and $t = 2500$s

FIGURE 6. Numerical results: interface evolution at different times

has been also tested for water solidification problem as water has different liquid-solid physical properties. The discrepancies between experimental and numerical results have been reduced, specially for large simulation times.

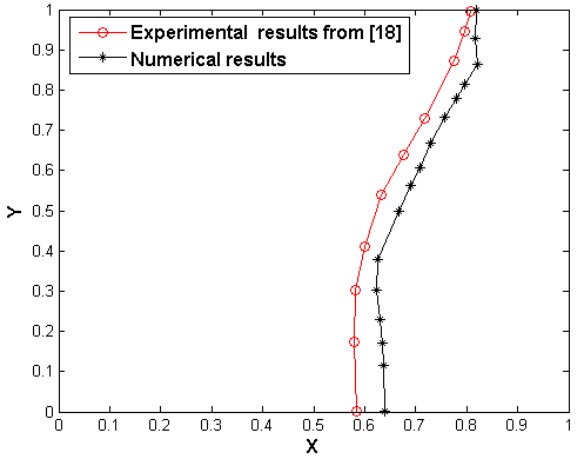

b) Numerical results from this work and experimental results from [18] at $t = 2500$s

FIGURE 7. Numerical results: interface evolution at different times

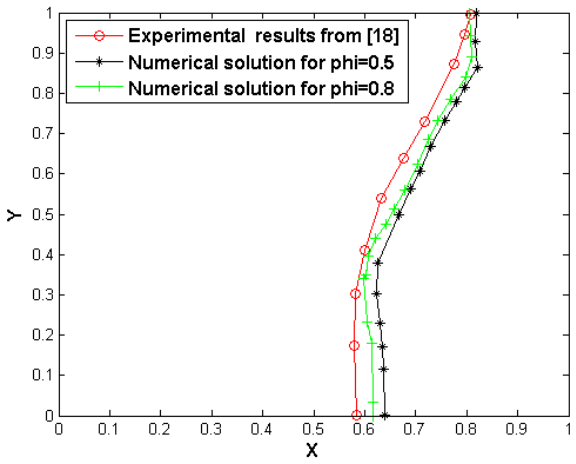

FIGURE 8. A cross section $z = 0.5$ of the two fronts $\phi = 0.5$ and $\phi = 0.8$

Our numerical results confirm that phase change problems with convection are very sensitive to mesh size. This was clearly demonstrated in the cell number and form of pure gallium melting problem. It would be very interesting to investigate the mesh dependence of water solidification in the three-dimensional case. This will be the object of a future work where the performance of time-dependent anisotropic mesh adaptation will be analyzed for these challenging problems.

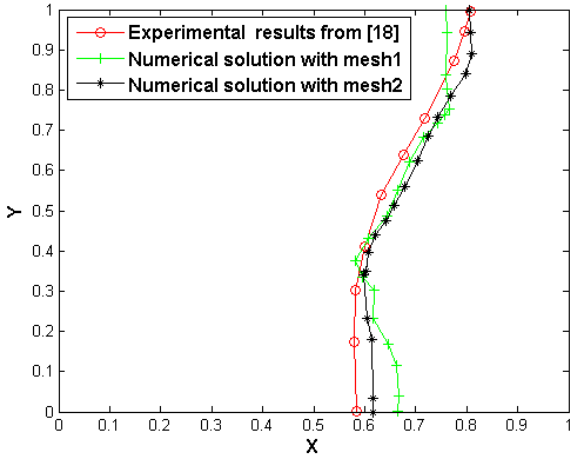

FIGURE 9. A cross section $z = 0.5$ of the front $\phi = 0.8$ obtained with two different meshes: mesh1=20^3, and mesh2=30^3.

Acknowledgments

The authors wish to acknowledge the financial support of Natural Sciences and Engineering Research Council of Canada (NSERC) and research funds of Campus Saint-Jean.

References

[1] J. Banaszek, Y. Jaluria, T. A. Kowalewski, and M. Rebow. Semi-Implicit FEM Analysis Of Natural Convection In Freezing Water. *Num. Heat Transfer, Part A*, 36:449–472, 1999.

[2] Y. Belhamadia, A. Fortin, and É. Chamberland. Anisotropic Mesh Adaptation for the Solution of the Stefan Problem. *Journal of Computational Physics*, 194 (1):233–255, 2004.

[3] Y. Belhamadia, A. Fortin, and É. Chamberland. Three-Dimensional Anisotropic Mesh Adaptation for Phase Change Problems. *Journal of Computational Physics*, 201(2):753–770, 2004.

[4] Y. Belhamadia, A. Kane, and A. Fortin. A Mixed Finite Element Formulation for Solving Phase Change Problems with Convection. In *Proceedings of the 20th Annual Conference of the CFD Society of Canada*, 2012.

[5] A. D. Brent, V. R. Voller, and K. J. Reid. Enthalpy-porosity technique for modeling convection-diffusion phase change: Application to the melting of a pure metal. *Numerical Heat Transfer*, 13(3):297–318, 1988.

[6] F. Brezzi and M. Fortin. *Mixed and Hybrid Finite Element Methods*. Springer-Verlag, 1991.

[7] A. El Maliki and R. Guénette. Efficient Preconditioning Techniques for Finite-Element Quadratic Discretization Arising from Linearized Incompressible Navier–Stokes Equations. *International Journal for Numerical Methods in Fluids*, 63(12):1394–1420, 2010.

[8] Katherine J. Evans and Dana A. Knoll. Temporal accuracy analysis of phase change convection simulations using the JFNK-SIMPLE algorithm. *International Journal for Numerical Methods in Fluids*, 55(7):637–653, 2007.

[9] Katherine J. Evans, D. A. Knoll, and Michael Pernice. Development of a 2-d algorithm to simulate convection and phase transition efficiently. *J. Comput. Phys.*, 219:404–417, November 2006.

[10] W. F. Florez, H. Power, and F. Chejne. Numerical solution of thermal convection problems using the multidomain boundary element method. *Numerical Methods for Partial Differential Equations*, 18(4):469–489, 2002.

[11] A. Fortin and Y. Belhamadia. Numerical Prediction of Freezing Fronts in Cryosurgery: Comparison with Experimental Results. *Comput. Methods Biomech. Biomed. Eng.*, 8(4):241–249, 2005.

[12] Marilena Giangi, Fulvio Stella, and Tomasz A. Kowalewski. Phase change problems with free convection: Fixed grid numerical simulation. *Comput Visual Sci*, 2:123–130, 1999.

[13] Marilena Giangi, Tomasz A. Kowalewski, Fulvio Stella, and Eddie Leonardi. Natural convection during ice formation: Numerical simulation vs. experimental results. *Computer Assisted Mechanics and Engineering Sciences*, 7:321–342, 2000.

[14] S. C. Gupta. A moving grid numerical scheme for multi-dimensional solidification with transition temperature range. *Computer Methods in Applied Mechanics and Engineering*, 189(2):525 – 544, 2000. ISSN 0045-7825.

[15] N. Hannoun, V. Alexiades, and T. Z. Mai. A reference solution for phase change with convection. *International Journal for Numerical Methods in Fluids*, 48 (11):1283–1308, 2005.

[16] Noureddine Hannoun, Vasilios Alexiades, and Tsun Zee Mai. Resolving the controversy over tin and gallium melting in a rectangular cavity heated from the side. *Numerical Heat Transfer B*, 44:253–276, 2003.

[17] T. A. Kowalewski and M. Rebow. An Experimental Benchmark for Freezing Water in the Cubic Cavity. In *Advances in Computational Heat Transfer, Begel House Inc., New York*, pages 149–156, 1998.

[18] T. A. Kowalewski and M. Rebow. Freezing of water in a differentially heated cubic cavity. *International Journal of Computational Fluid Dynamics*, 11(3-4): 193–210, 1999.

[19] M. A. Rady and A. K. Mohanty. Natural convection during melting and solidification of pure metals in a cavity. *Numerical Heat Transfer, Part A: Applications*, 29(1):49–63, 1996.

[20] A.A. Samarskii, P.N. Vabishchevich, O.P. Iliev, and A.G. Churbanov. Numerical simulation of convection/diffusion phase change problems–a review. *International Journal of Heat and Mass Transfer*, 36(17):4095 – 4106, 1993.

[21] Fulvio Stella and Marilena Giangi. Melting of a pure metal on a vertical wall: Numerical simulation. *Numerical Heat Transfer Part A-applications*, 38:193–208, 2000.

[22] C. Swaminathan and V. Voller. A general enthalpy method for modeling solidification processes. *Metallurgical and Materials Transactions B*, 23:651–664, 1992.

[23] R. Viswanath and Y. Jaluria. A comparison of different solution methodologies for melting and solidification problems in enclosures. *Numerical Heat Transfer, Part B: Fundamentals*, 24(1):77–105, 1993.

[24] V. R. Voller, M. Cross, and N. C. Markatos. An enthalpy method for convection/diffusion phase change. *International Journal for Numerical Methods in Engineering*, 24(1):271–284, 1987.

[25] V.R. Voller and C. Prakash. A fixed grid numerical modelling methodology for convection-diffusion mushy region phase-change problems. *International Journal of Heat and Mass Transfer*, 30(8):1709 – 1719, 1987.

University of Alberta, Campus Saint-Jean & Mathematical Department, Edmonton, Alberta, Canada.,
E-mail: Corresponding author: youssef.belhamadia@ualberta.ca

University of Ottawa, Department of Mathematics and Statistics, Ottawa, Ontario, Canada.
E-mail: akane@giref.ulaval.ca

Université Laval, Département de mathématiques et de statistique, Québec, Québec, Canada
E-mail: afortin@giref.ulaval.ca